Synthesis of Organic–Inorganic Hybrid Polymeric Nanocomposites for the Hard Coat Application

Chuan Hsiao Shu,[1] Hau-Chun Chiang,[1] Raymond Chien-Chao Tsiang,[1] Ta-Jo Liu,[2] Jeng-Jaw Wu[3]

[1]*Department of Chemical Engineering, National Chung Cheng University, Chiayi, Taiwan, Republic of China*
[2]*Department of Chemical Engineering, National Tsing Hua University, Hsin Chu, Taiwan, Republic of China*
[3]*Crest Technology Co., Ltd., Hsin Chu, Taiwan, Republic of China*

Received 6 April 2006; accepted 11 September 2006
DOI 10.1002/app.25477
Published online in Wiley InterScience (www.interscience.wiley.com).

ABSTRACT: An organic–inorganic hybrid polymeric nanocomposite has been synthesized for making UV-curable hard coats. This nanocomposite consists of nano-sized colloidal silica functionalized with vinyltriethoxysilane (VTES) and dendritic acrylic oligomers (DAO) which have been formed earlier via a reaction of ethylenediamine (EDA) with trimethylopropane triacrylate (TMPTA). Applied as a hard coat on top of a polyethylene terephthalate (PET) film, this nanocomposite has a short UV-cure time and the cured coat has an enhanced thermal decomposition temperature (T_d), 89–90% transparency, increased hardness up to 3H, better adhesion up to 4B, and a flat surface with a root mean square roughness of 2–4 nm. The preparation as well as the characterization of the constituting species and the final hybrid are described in detail. © 2006 Wiley Periodicals, Inc. J Appl Polym Sci 103: 3985–3993, 2007

Key words: hybrid; nanocomposites; UV-curable; hard coat

INTRODUCTION

In recent years, UV-curable hard coatings that can be applied to the plastic substrate for the protection purpose have gained extensive interest.[1–12] Coatings that are abrasion resistant and require short cure time are much desired. The acrylic monomer/oligomer is an important UV-curable resin widely used for coatings because of its excellent optical properties and easy processability.[2] However, the lack of hardness of the cured resin often results in scratch damages on the surface. Among various hardness improvement method, the making of organic–inorganic hybrid materials has received great attention.[1,3,13–15] Such hybrid materials often exhibit markedly improved mechanical properties and weatherability arising from the contribution of the inorganic elements. In particular, the acrylate/silica hybrid material has found a great potential in use as a transparent protecting film for various optical panel displays. Nevertheless, the incompatibility between the organic and inorganic phase causes poor dispersion of silica particles in the acrylate matrix and makes a direct blending of acrylate and silica particles impossible.

Two ways for preparing acrylate/silica hybrid have been studied over the past years. The first involves the polymerization of acrylic monomers in the presence of an ethenic monomer containing silicon alkoxides in its molecular structure, forming the $Si(OR)_3$-containing polyacrylate. This polyacrylate undergoes then a condensation reaction with tetraethoxysilane (TEOS), thus resulting in an acrylate/(silica particles) hybrid.[16,17] However, the nonuniformity of the size of the *in situ* formed silica particles often causes deleterious optical effects. The other way is to copolymerize acrylic monomers with functionalized silica particles of an uniform size.[8,18] While the rate of copolymerization (i.e., the cure rate) is not fast, the transparency requirement of the protecting film often necessitates the choice of the latter way concurrent with the use of nano-sized silica particles.

In the work described here, a novel method was used for preparing an acrylate/(silica nanoparticles) hybrid material that could be cured quickly. First, silica nanoparticles were functionalized with vinyltriethoxysilane (VTES) to afford reactive groups to the nanoparticles. Next, these functionalized nanoparticles were mixed with dendritic acrylic oligomers (DAO) with multiple reactive groups to make a thin film on top of a plastic substrate. After a short UV-cure time, the cured film exhibited excellent transparency, adhesion, haze, and hardness characteristics.

EXPERIMENTAL

Materials

Trimethylolpropane triacrylate (TMPTA), vinyltriethoxysilane (VTES), 1-hydroxycyclohexyl phenyl

Correspondence to: R. C. Tsiang (chmcct@ccu.edu.tw).
Contract grant sponsor: National Science Council of the Republic of China; contract grant number: NSC93-2622-E-007-009.

TABLE I
Compositions of VTES-Functionalized Silica

Sample	VTES/silica (*R*)	VTES (g)	Colloidal silica (g)[a]	H_2O (g)
VT01	0.1	0.9	30	0.852
VT02	0.2	1.8	30	1.705
VT03	0.3	2.7	30	2.557
VT04	0.4	3.6	30	3.410
VT05	0.5	4.5	30	4.547

[a] 30 wt % silica in isopropanol.

ketone (HCPK, Irgacure 184), and hydrochloric acid with a concentration of 0.1 mol/L were purchased from Aldrich Chemical and used without further purification. Ethylenediamine (EDA) and isopropanol were purchased from Fluka. Colloidal nano-sized silica of a diameter of 10–12 nm was purchased from (Echo Nano-bio, Taiwan) as a clear suspension in isopropanol with a solid content of 30%. Nonionic fluorosurfactant FC-4430 was purchased from 3M Company (St. Paul, MN).

Synthesis

VTES, H_2O, HCl, and silica nanoparticles were added into a three-necked flask equipped with a magnetic stirrer. The hydrolysis of VTES and the condensation of silanols were carried out simultaneously at 75°C for 2 h under various formulations (shown in Table I) to produce the functionalized silica (V-silica) solution. The number of moles of water was ten times that of VTES, and 0.2–0.3 g of HCl was added to maintain a pH at 3–4. The reaction is shown in Scheme 1.

In another three-necked flask, TMPTA (0.1 mol) was dissolved in IPA (12 g) before the addition of EDA (0.02 mol). This mixture was kept at 30°C for 6 h with stirring to yield the dendritic acrylic oligomers

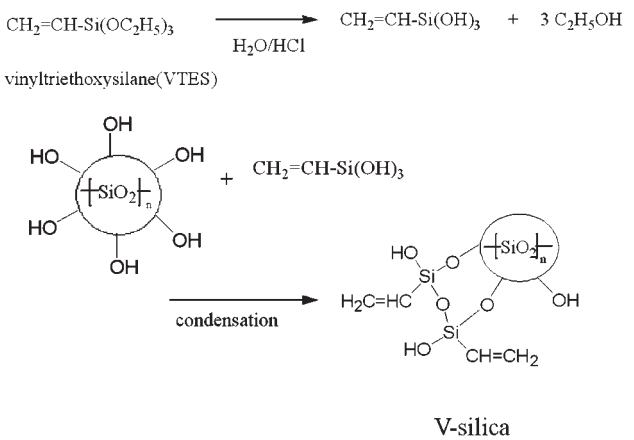

Scheme 1 Functionalization of silica nanoparticles.

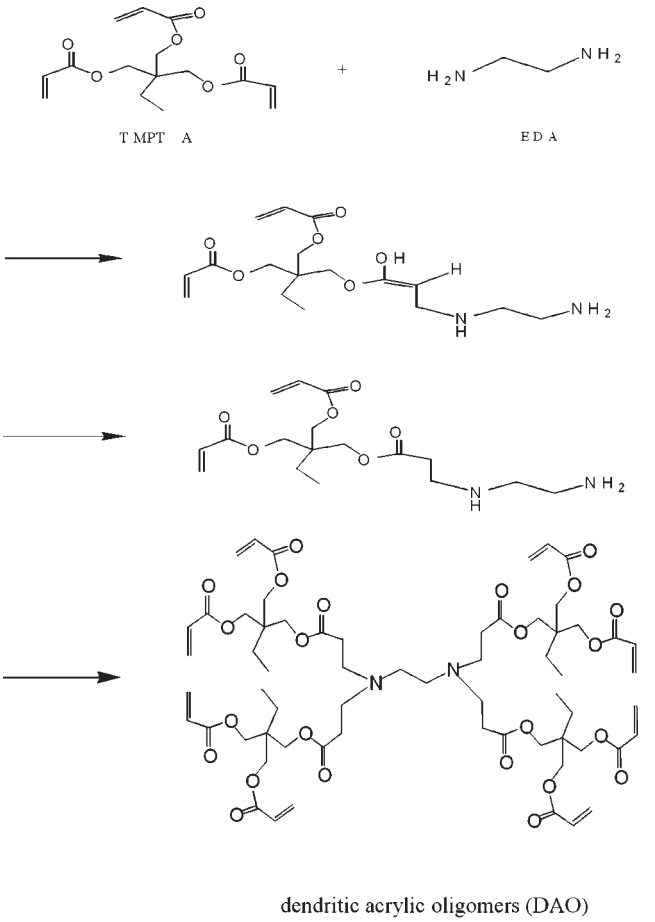

Scheme 2 Formation of dendritic acrylic oligomers.

based on the method proposed previously by Xu et al.[2] The reaction is shown in Scheme 2.

The V-silica solution and the oligomer solution were then mixed at various weight ratios in the presence of 25 wt % diluting TMPTA, 4 wt % Irgacure

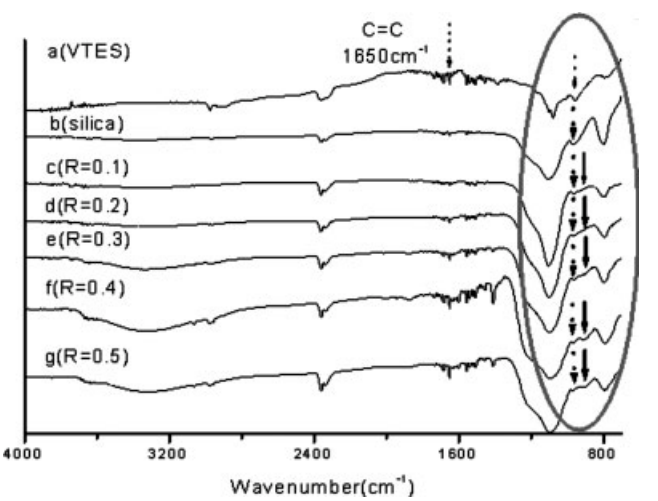

Figure 1 FTIR spectra of VTES, silica, and sample VT01-VT05 at various VTES/silica weight ratio (*R*).

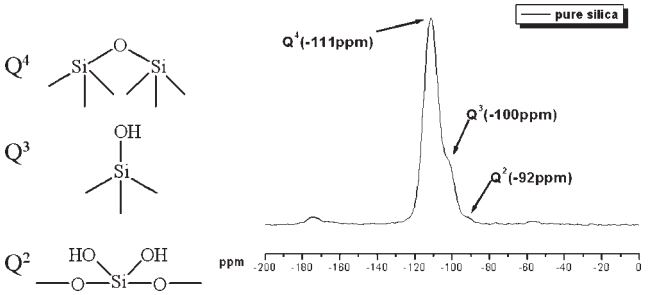

Figure 2 ^{29}Si solid-state NMR spectrum of pristine silica.

184, and 0.03 wt % FC-4430. This acrylate/(silica nanoparticles) hybrid mixture was roller coated on a polyethylene terephathalate (PET) film with a coating thickness of 4 mm and put under UV irradiation (wavelength: 365 nm; power: 240 mW/cm^2) for curing. The curing lasted for 60 s. The cured film was analyzed for its optical, thermal, and physical characteristics.

Measurements

The molecular structures of acrylic oligomers were determined from ^{1}H- and ^{13}C-NMR (Varian-Unity INOVA-500 MHz) and ^{29}Si-SNMR (BRUKER AMX 400 spectrometer) spectra of samples in $CDCl_3$ at 30°C. The functional groups of V-silica were analyzed with a Shimadzu SSU-8000 FTIR spectrophotometer. The molecular structure was determined with the use of JEOL-SX102A GC/LC/MS mass spectrometer (MS). Scanning electron microscope (SEM) images were obtained on a Hitachi S4800 Type I SEM system for sample deposited onto a TEM grid (copper, 3.0 mm, 200 mesh, and coated with a Formvar film). The thermal behavior of the polyacrylate/(silica nanoparticles) hybrid material (8–10 mg) was evaluated with a thermogravimetric analyzer (TGA 2050, TA Instruments) in an aluminum pan with a heating rate of 20°C/min from room temperature to 900°C under nitrogen at a flow rate of 20 mL/min. Differential scanning calorimeter (DSC) analysis was done on a modulated DSC2910 (TA Instruments) under nitrogen at a flow rate of 80 mL/min. The atomic force microscope (AFM) height-mode micrographs were obtained from the Quesant Universal SPM Instruments, using a silicon-nitride-based cantilever coated with magnetic film as the AFM tip. The hardness of the film was measured in accord with ASTM D3363 method using a pencil meter. The adhesion of the hybrid material to PET was measured by ASTM D3359 method. The transparency and haze were examined with a Nippon Denshoku 300A instrument following the ASTM D1003 method.

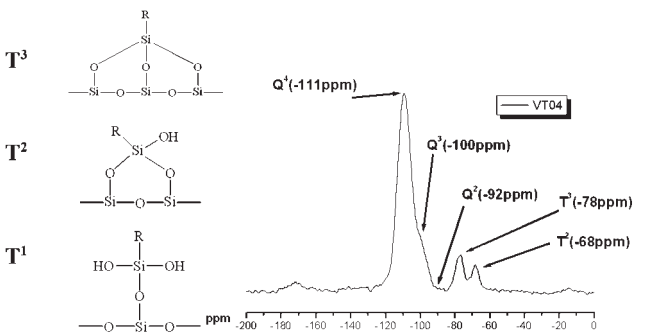

Figure 3 ^{29}Si solid-state NMR spectra of functionalized silica VT04.

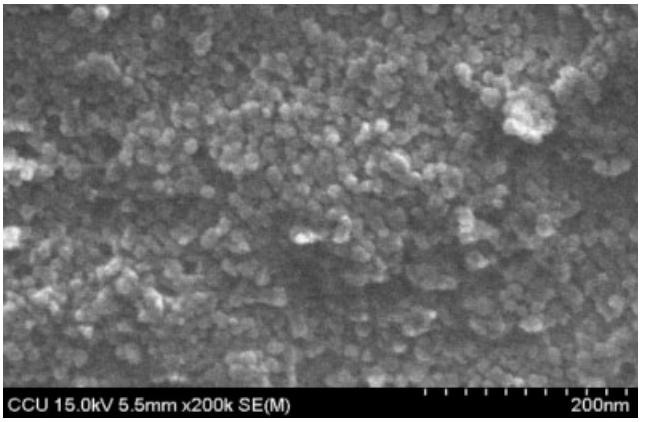

Figure 4 SEM image of pristine silica (scale bar = 200 nm).

RESULTS AND DISCUSSION

Functionalization of silica nanoparticles with VTES

FTIR spectra shown in Figure 1 indicate that the amount of silanols on the surface of silica (peak at 962 cm^{-1}) decreased when silica nanoparticles were functionalized by VTES. However, the amount of silanols generated by the hydrolysis of VTES (peak at

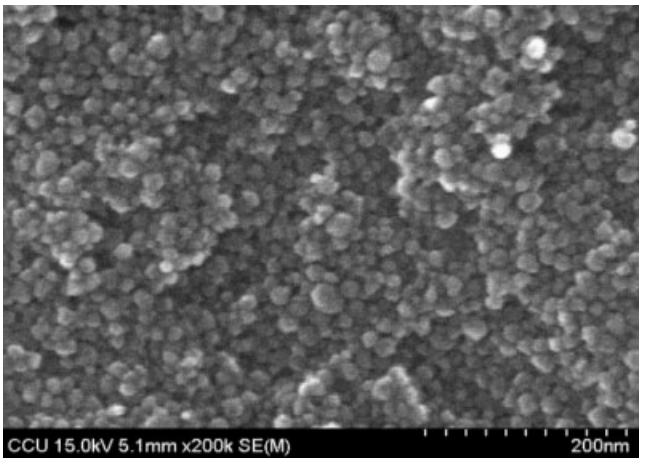

Figure 5 SEM image of VTES-functionalized silica VT04 (scale bar = 200 nm).

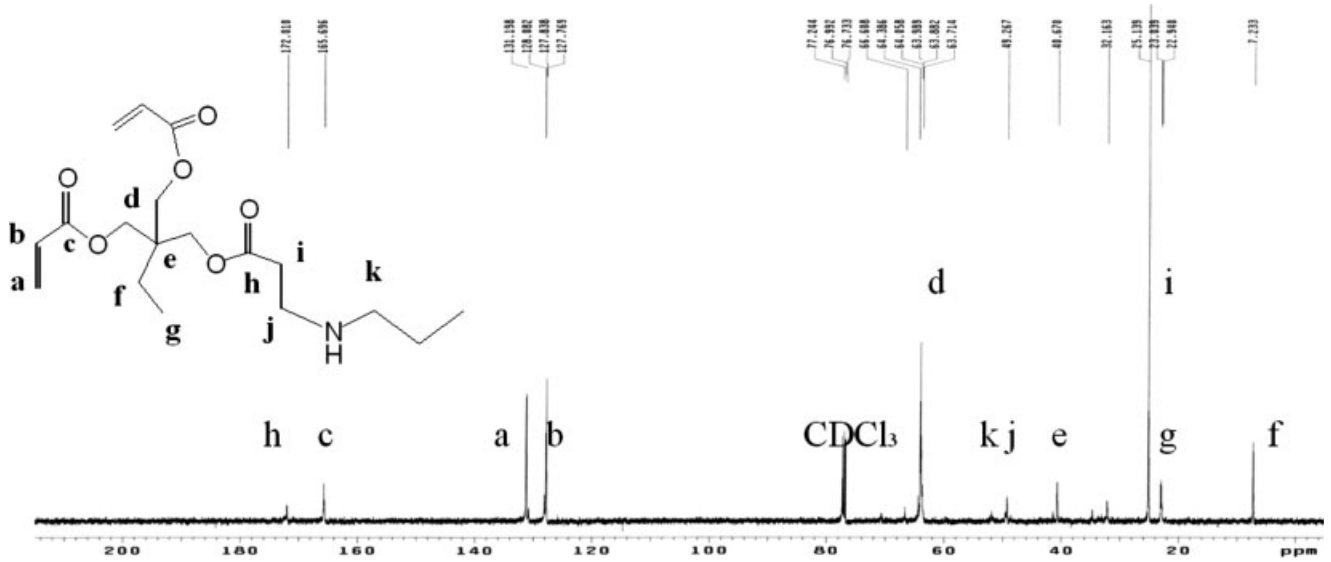

Figure 6 ^{13}C-NMR spectrum of the acrylic oligomer.

912 cm^{-1}) was minimal unless the amount of VTES added was more than 0.4 VTES/silica weight ratio. This observation suggests that the inherent silanols on the surface of silica nanoparticles were completely consumed by the hydrolyzed VTES at that weight ratio.

The ^{29}Si-SNMR spectrum of pristine silica is shown in Figure 2. The Q^3 and Q^2 peaks indicate the existence of inherent silanols on the surface of the silica nanoparticles. After the functionalization with VTES by a 0.4 weight ratio (Fig. 3), Q^3 and Q^2 peaks diminished, thus verifying the reaction of silanols with VTES. In the meanwhile, two new peaks, T^3 and T^2 were generated indicating that the VTES was either triply bonded or doubly bonded to silica nanoparticles. The singly bonded VTES, T^1, was not observed presumably because the amount of VTES (at $R = 0.4$) was not big enough. These ^{29}Si-SNMR spectrums thus corroborate the successful functionalization of silica nanoparticles by VTES.

At a 2×10^5 times magnification, the SEM images (Figs. 4 and 5) clearly show that the size of silica nanoparticles increased after the VTES functionalization. This increase was ascribed to the inclusion of VTES into the siloxane network structure.

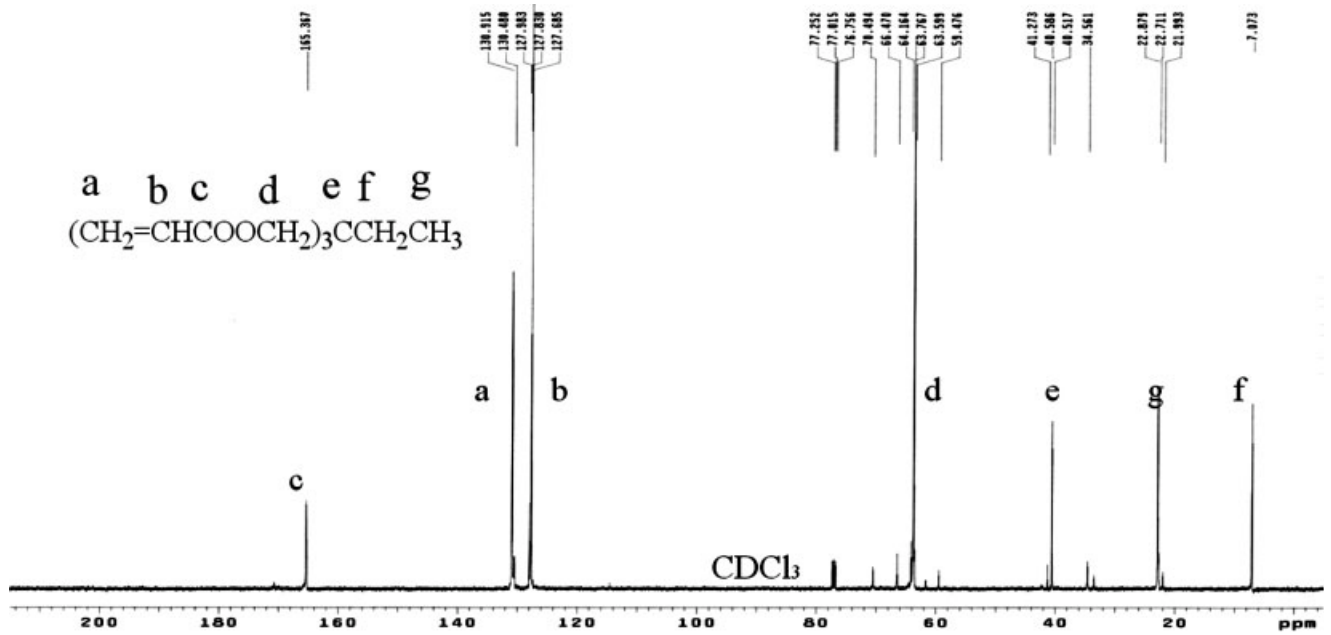

Figure 7 ^{13}C-NMR spectrum of TMPTA.

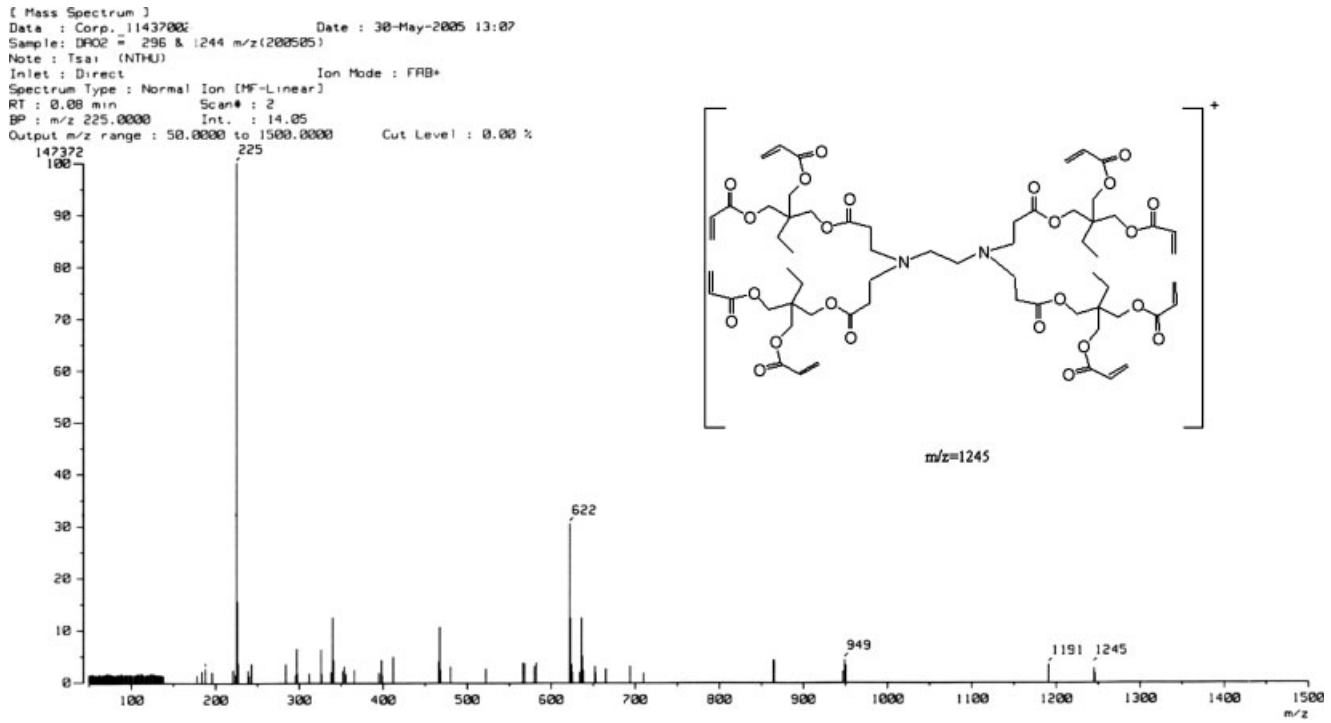

Figure 8 Mass spectrum of TMPTA.

Formation of the dendritic acrylic oligomers

Each dendritic oligomer molecule has eight ethenic double bonds and its molecular structure was verified on the basis of a comparison of the ^{13}C-NMR spectrum (Fig. 6) of the acrylic oligimer with that (Fig. 7) of TMPTA. Peaks at $\delta_b = 127.8$ and $\delta_a = 130.198$ diminished after the reaction of TMPTA with EDA as a result of the consumption of ethenic double bonds. Furthermore, the generation of three new peaks, δ_h, δ_i, and δ_j, corroborated the reaction of EDA with the ethenic double bonds of TMPTA. However, it was difficult to ascertain from these spectra how many TMPTA molecules each EDA reacted with. Therefore, MS was used to determine the molecular weight of the acrylic oligomer. With the use of the fast atom bombardment mass spectrometer (FAB-MS), the mass spectrum (Fig. 8) clearly identified the parent ion of $m/z = 1245$ in accord with the expected molecular structure—each dendritic oligomer molecule consisted of four TMPTA and one EDA and had eight ethenic double bonds. Other fragment ions having $m/z = 949$, 622, and 225 were also identified as the fragmental derivatives of the oligomer (Scheme 3).

Compositions and properties of hybrid acrylate/(silica nanoparticles) materials

As listed in Table II are the compositions of various hybrid acrylate/(V-silica) coating formulations. The decomposition temperatures (T_d) of various polyacrylate/(silica nanoparticles) hybrid materials were determined with TGA and data are summarized in Table III. For comparison, both pristine silica and the functionalized silica were tried for making the organic–inorganic hybrid. Shown in Figures 9 and 10 are T_d data from the hybrid materials composed of various amount of pristine silica and V-silica, respectively. Both silica caused an increase in T_d, but V-silica caused more increase. However, for pristine silica a maximum T_d occurred at a silica content of

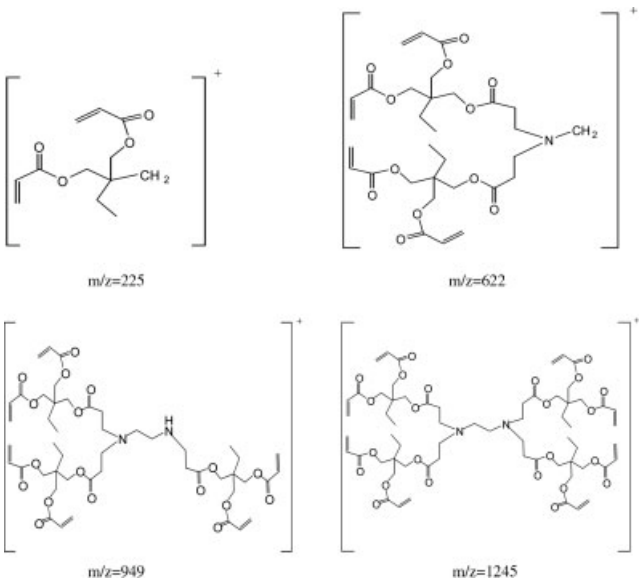

Scheme 3 Parent and fragment ions of TMPTA derivatives.

TABLE II
Compositions of Various Hybrid Materials (wt %)

Series	VTES/silica	Sample	V-silica	DAO	TMPTA	Initiator[a]	Surfactant[b]
A	0	A-25	10	65	25	4	0.03
	0	A-50	20	55	25	4	0.03
	0	A-75	30	45	25	4	0.03
B	0	A-100	40	35	25	4	0.03
	0	A-125	50	25	25	4	0.03
	0.4	B-25	10	65	25	4	0.03
	0.4	B-50	20	55	25	4	0.03
	0.4	B-75	30	45	25	4	0.03
C	0.4	B-100	40	35	25	4	0.03
	0.4	B-125	50	25	25	4	0.03
	0.5	C-25	10	65	25	4	0.03
	0.5	C-50	20	55	25	4	0.03
	0.5	C-75	30	45	25	4	0.03
S	0.5	C-100	40	35	25	4	0.03
	0.5	C-125	50	25	25	4	0.03
	0.4	S-04	50	25	25	4	0.03
	0.5	S-05	50	25	25	4	0.03
	0.6	S-06	50	25	25	4	0.03
	0.7	S-07	50	25	25	4	0.03
	0.8	S-08	50	25	25	4	0.03

[a] Initiator/(V-silica + DAO + TMPTA) (wt %).
[b] Surfactant/(V-silica + DAO + TMPTA) (wt %).

about 5 wt % and any further increase beyond 5 wt % led to a drop of T_d. This observation indicated that the incompatibility became significant when the amount of pristine silica exceeded a certain limit and thus resulted in an inferior crosslinking reaction in the organic matrix.

TABLE III
T_d and Residue Weight of Cured Hybrid Materials

Series	VTES/silica	Sample	Silica (wt %)[a]	T_d (°C)[b]	Residue weight (%)[c]
PET			0		
DAO			0	226.51	4.4
A	0	A-25	2.50	266.04	6.385
	0	A-50	5.00	279.76	9.369
	0	A-75	7.50	260.54	10.34
	0	A-100	10.00	253.4	14.31
	0	A-125	12.50	239.18	19.39
B	0.4	B-25	2.50	291.55	5.521
	0.4	B-50	5.00	294.13	8.743
	0.4	B-75	7.50	288.65	10.5
	0.4	B-100	10.00	283.42	13.73
	0.4	B-125	12.50	286.09	22.45
C	0.5	C-25	2.50	NA	NA
	0.5	C-50	5.00	NA	NA
	0.5	C-75	7.50	NA	NA
	0.5	C-100	10.00	NA	NA
	0.5	C-125	12.50	276.66	24.83
S	0.2	S-02	12.50	267.03	22.06
	0.3	S-03	12.50	274.2	25.6
	0.4	S-04	12.50	296.09	22.45
	0.5	S-05	12.50	276.66	24.83
	0.6	S-06	12.50	282.74	25.35
	0.7	S-07	12.50	270.52	25.03
	0.8	S-08	12.50	270.87	25.1

[a] Theoretical values based on the assumption that only inorganic moieties were present at 900°C.
[b] Temperature at 5 wt % weight loss.
[c] Experimental results from TGA at 900°C.

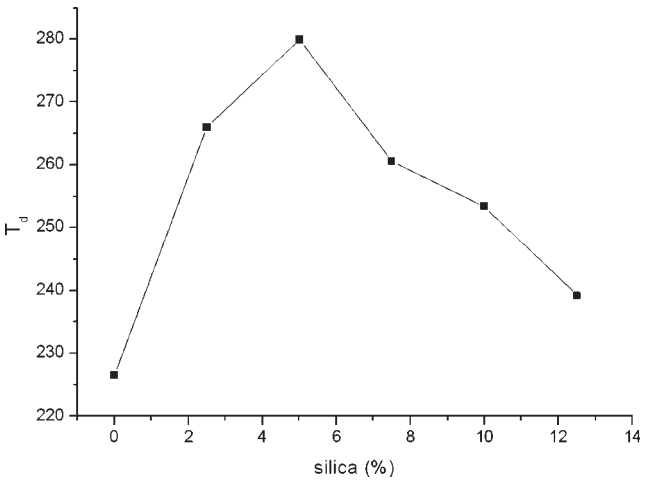

Figure 9 Plot of T_d versus silica content for hybrid materials.

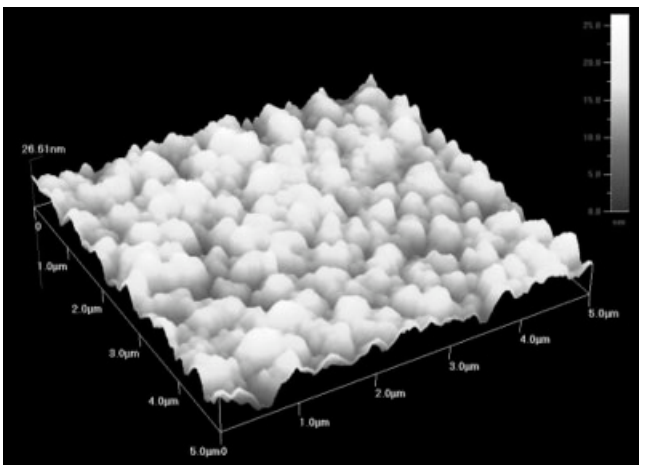

Figure 11 AFM image of surface of coated B-125 on PET film.

The DSC thermograms of the acrylic oligomer and various hybrid samples have been examined in the temperature range from 50 to 200°C. No T_g was ever observed within this temperature range because the UV-curing reaction among the dendritic oligomer, V-silica, and TMPTA produced a crosslinked network polymer with an enhanced T_g beyond 200°C. This T_g would be difficult to measure because it was too close to T_d.

The surface of the cured film was examined with AFM. Although the hybrid materials had surface flatness inferior to the neat acrylic oligomer because of the silica particles, the root mean square roughness (RMS) are still within the acceptable range of 2–4 nm. Shown in Figure 11 is the AFM microgram of the surface of B125 sample (containing V-silica) coated on the PET substrate. To contrast, the AFM microgram of A125 sample (containing pristine silica) on the PET substrate is shown in Figure 12. Pristine silica conglomerated while the V-silica exhibited a flatter surface owing to its higher compatibility.

Data for various hybrid sample films coated on PET substrate are listed in Table IV. All had 89–90% transparencies with or without silica nanoparticles. Silica nanoparticles, as employed in these samples, did not have deleterious effects on transparency. This was because the refractive index of silica nanoparticles (1.45 as shown in Refs. 19 and 20) was similar to that of polyacrylate (1.47–1.48 as shown in Ref. 21) and TMPTA (1.47 as shown in Ref. 22) and in the meanwhile, the size of silica nanoparticles was too small to cause any significant light scattering. It was also worthy to notice that the transparency of any hybrid sample on the PET film was higher than that of the PET film alone (88.2%). Apparently, the smaller refractive index of silica nanoparticles and polyacrylate than PET ($n_{\text{silica}} = 1.45$, $n_{\text{PET}} = 1.53$) enhanced the

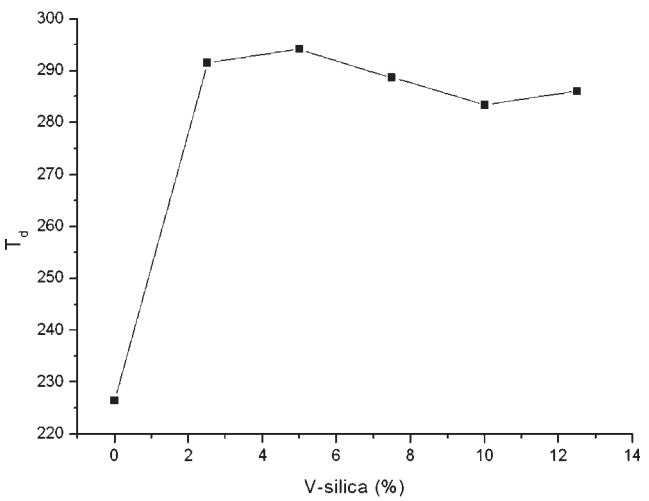

Figure 10 Plot of T_d versus V-silica content for hybrid materials.

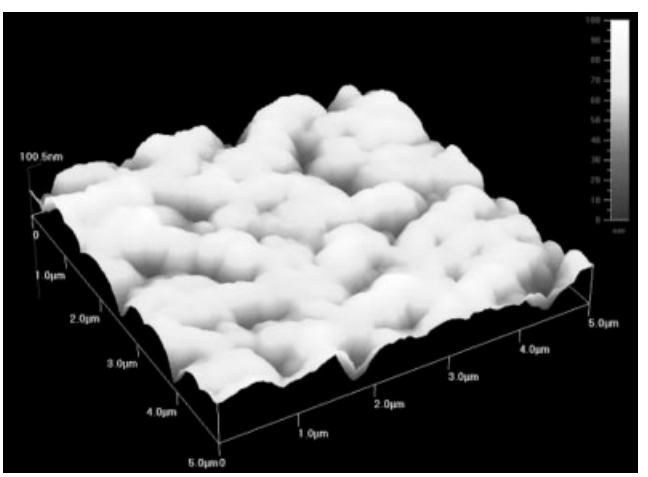

Figure 12 AFM image of surface of coated A-125 on PET film.

TABLE IV
Properties of Cured Hybrid Thin Films

Sample	TT (%)[a]	Haze (%)	Hardness[b]	Adhesion[c]	RMS (nm)[d]	Ra (nm)[e]
PET	88.2	4.9	HB		9.173	7.316
DAO	89.5	5.5	3H	0B	1.427	1.14
A-25	89.5	6.5	3H	1B	NA	NA
A-50	89.5	6	3H	1B	NA	NA
A-75	89.7	5.6	2H	3B	NA	NA
A-100	89.7	5.4	2H	4B	5.38	4.298
A-125	89.8	8	2H	4B	15.83	12.31
B-25	89.5	5.7	3H	0B	NA	NA
B-50	89.5	5.4	3H	1B	NA	NA
B-75	89.6	5.6	3H	2B	NA	NA
B-100	89.5	5.2	2H	2B	3.653	2.925
B-125	89.5	5.6	2H	3B	3.842	3.114
C-25	89.5	5.4	3H	1B	NA	NA
C-50	89.6	5.5	3H	1B	NA	NA
C-75	89.8	5.2	2H	2B	NA	NA
C-100	89.7	5.2	2H	3B	2.32	1.867
C-125	89	3.8	3H	4B	NA	NA
S-04	89.5	5.6	2H	3B	3.842	3.114
S-05	89	3.8	3H	4B	6.12	4.429
S-06	89.7	5.6	2H	4B	NA	NA
S-07	89.7	5.7	3H	4B	NA	NA
S-08	89.6	5.6	2H	4B	NA	NA

[a] TT, Transparency.
[b] The degree of hardness: 3H > 2H > HB.
[c] Adhesion: 4B > 3B > 2B > 1B > 0B.
[d] RMS, root mean square roughness of prepared thin films.
[e] Ra, average roughness of prepared thin films.

penetration of light. Therefore, it was conceivable that the transparency could be further enhanced provided other substances with better optical properties were chosen as the substrate, e.g., an optical PET.

The hardness of the hybrid materials on PET film were measured and data are tabulated in Table IV. Compared with the hardness of PET film alone (HB), the hybrid samples on PET film exhibited better hardness as high as 3H. This observation was not unexpected because silica nanoparticle was a major contributor for the improvement in hardness. However, the fact that the hardness did not vary significantly to the amount of silica nanoparticles suggested the existence of a trade-off between the hardness and the compatibility.

As seen from Table IV, although the low degree of light scattering led to very low haze in the hybrid films, the hybrid films with V-silica nanoparticles had lower haze (3.8–5.7) than those with pristine silica nanoparticles (5.4–8). This could be attributed to the reason that V-silica nanoparticles had higher compatibility with the organic acrylate phase and thus had less particle aggregation which would adversely affects the haze.

The hybrid material adhered better to the PET substrate than the acrylate oligomer. Adhesion data for all samples are tabulated in Table IV. Generally, the adhesion of the hybrid material increased with an increase in the silica content because the inclusion of inorganic elements alleviated the extent of shrinkage and maintained better contact between the coating and the substrate.

CONCLUSIONS

An UV-curable organic–inorganic hybrid nanocomposite, consisting of dendritic acrylic oligmers and functionalized silica nanoparticles, possesses enhanced properties when applied as a hard coat on top of the PET film. The UV-cure time is short and the cured coat has an increased hardness up to 3H.

References

1. Gigant, K.; Posset, U.; Schottner, G. J Sol-Gel Sci Technol 2003, 26, 369.
2. Xu, D.; Zhang, K.; Zhu, X. J Appl Polym Sci 2004, 92, 1018.
3. Lewis, L. N.; Katsamberis, D. J Appl Polym Sci 1991, 42, 1551.
4. Fieberg, A.; Reis, O. Prog Org Coat 2002, 45, 239.
5. Yang, Y. Y.; Wu, Y. M.; Hu, H.; Tan, H. Y. Photogr Sci Photochem 2002, 20, 230.
6. Fisher, E. A. Y. Photon Spectra 2003, 37, 82.

7. Lin, D.; Kou, H. G.; Shi, W. F.; Yuan, H. Y.; Chen, Y. L. J Appl Polym Sci 2001, 82, 1637.
8. Wouters, M. E. L.; Wolfs, D. P.; van der Linde, M. C.; Hovens, J. H. P.; Tinnemans, A. H. A. Prog Org Coat 2004, 51, 312.
9. Que, W.; Zhang, Q. Y.; Chan, Y. C.; Kam, C. H. Compos Sci Technol 2003, 63, 347.
10. Schotiner, G.; Rose, K.; Posset, U. J Sol-Gel Sci Technol 2003, 27, 71.
11. Lindawu, Y. L.; Tan, G. H.; Zeng, X. T.; Li, T. H.; Chen, Z. J Sol-Gel Sci Technol 2006, 38, 85.
12. Kuraoka, K.; Ueda, T.; Sato, M.; Okamoto, T.; Yazawa, T. J Mater Sci 2005, 40, 3577.
13. Daniels, M. W.; Francis, L. F. J Colloid Interface Sci 1998, 205, 191.
14. Medford, F. G.U.S. Pat. 5,607,729(1997).
15. Yu, Y. Y.; Chen, C. Y.; Chen, W. C. Polymer 2003, 44, 593.
16. Mammeri, F.; Rozes, L.; Bourhis, E. L.; Sanchez, C. J Eur Ceram Soc 2006, 26, 267.
17. Coltrain, B. K.; Landry, C. J. T.; O'Reilly, J. M.; Chamberlain, A. M.; Rakes, G. A.; Sedita, J. S.; Kelts, L. W.; Landry, M. R.; Long, V. K. Chem Mater 1993, 5, 1445.
18. Rubio, E.; Almaral, J.; Ramírez-Bon, C. R.; Castaîno, B. V.; Rodríguez, V. Opt Mater 2005, 27, 1266.
19. Saitoh, K.; Koshiba, M. Opt Express 2005, 13, 267.
20. Mihi, A.; Miguez, H.; Rodriguez, I.; Rubio, S.; Meseguer, F. Phys Rev B 2005, 71, 125131.
21. Brandrup, J.; Immergut, E. H.; Grulke, E. A.; Polymer Handbook, 4th ed. p VI-580.
22. Material safety data sheet of TmPTA from Sigma-Aldrich: (St. Louis, MO) 2006.